

# Winding up a finite size holographic superconducting ring beyond Kibble-Zurek mechanism

Chuan-Yin Xia<sup>1,2</sup> and Hua-Bi Zeng<sup>1</sup>

email: hbzeng@yzu.edu.cn

<sup>1</sup> *Center for Gravitation and Cosmology, College of Physical Science and Technology, Yangzhou University, Yangzhou 225009, China and*

<sup>2</sup> *School of Science, Kunming University of Science and Technology, Kunming 650500, China*

We studied the dynamics of the order parameter and the winding numbers  $W$  formation of a quenched normal-to-superconductor state phase transition in a finite size holographic superconducting ring. There is a critical circumference  $\tilde{C}$  below it no winding number will be formed, then  $\tilde{C}$  can be treated as the Kibble-Zurek mechanism (KZM) correlation length  $\xi$  which is proportional to the fourth root of its quench rate  $\tau_Q$ , which is also the average size of independent pieces formed after a quench. When the circumference  $C \geq 10\xi$ , the key KZM scaling between the average value of absolute winding number and the quench rate  $\langle |W| \rangle \propto \tau_Q^{-1/8}$  is observed. At smaller sizes, the universal scaling will be modified, there are two regions. The middle size  $5\xi < C < 10\xi$  result  $\langle |W| \rangle \propto \tau_Q^{-1/5}$  agrees with a finite size experiment observation. While at  $\xi < C \leq 5\xi$  the the average value of absolute winding number equals to the variance of winding number and there is no well exponential relationship between the quench rate and the average value of absolute winding number. The winding number statistics can be derived from a trinomial distribution with  $\tilde{N} = C/(f\xi)$  trials,  $f \simeq 5$  is the average number of adjacent pieces that are effectively correlated.

Second order phase transition that traverses the critical point at a finite rate is a non-equilibrium process. Due to the relaxation time's divergence near critical point (critical slowing down), the formation of topological defects by taking into account finite speed of propagation of the relevant information was predicted by the Kibble-Zurek mechanism (KZM)[1–8]. The original idea of KZM is from Kibble's insight on the role of causality in structure formation in the early universe [1, 2]. Later, Zurek found that condensed-matter systems offer a test-bed to study the dynamics of symmetry breaking [3–5]. He firstly predicted the formation of independent regions with their average size controlled by the correlation length  $\xi$  at the point when the frozen time ends,  $\xi$  scales with the linear quench rate  $\tau_Q$  in which the phase transition is crossed as a universal power-law

$$\xi \propto \tau_Q^\alpha, \quad (1)$$

the power-law exponent  $\alpha = \nu/(1 + \nu z)$  is set by a combination of the dynamic and correlation-length (equilibrium) critical exponents denoted by  $z$  and  $\nu$ , respectively. By assuming the number of defects is proportion to the numbers of independent regions formed  $N$  and  $N \propto L^d/\xi^d$  ( $L$  is the size of the system,  $d$  is the dimensionality of the system), then the average density  $\tilde{n} = N/L^d$  of the resulting topological defects scales with the linear quench rate as a universal power-law

$$\tilde{n} \propto \tau_Q^{-d\alpha}, \quad (2)$$

this is the key prediction of KZM.

In 3D and 2D systems, the topological defects are usually vortex strings [9] and vortices [10, 11] respectively with zeroth order parameter inside the vortex cores. In a

1D system with real order parameter, kinks is the topological defects with zero order parameter in the center [12]. While in a 1D systems with a complex order parameter undergo a phase transition that breaks the  $U(1)$  gauge symmetry, winding numbers  $W = \oint_C d\theta/2\pi$  are expected to form but the amplitude of the order parameter keeps uniform[13, 14]. Numerical experiments in a quenched superfluid/superconductor have supported the KZM's key prediction of scaling in 3D [9], 2D [11, 15, 16] and 1 D [13, 14]. In laboratory, the Eq.(2) has also been confirmed in liquid crystals [17–19], <sup>3</sup>He superfluids [20, 21], Josephson junctions [22–25], thin-film superconductors [26, 27], a linear optical quantum simulator[28] and also in a strongly interacting Fermi superfluid [29]. Recently, Adolfo del Campo, etl found the universal statistics of topological defects formed in a quantum phase transition beyond KZM [30, 31], which has been confirmed by a 1D quantum simulation [32].

Despite the progress, few attention has been devoted to the case when the size of the system approaches the order of  $\xi$ . Except in experiment [33] the size effect results was reported in an Bose gases through a temperature quench of the normal-to-superfluid phase transition. Large size observation matches the KZM's prediction by using the mean field theory critical exponents  $z = 2, \nu = 1/2$ , where  $\langle |W| \rangle \propto \tau_q^{-1/8}$  at fixed  $C$  and  $\langle |W| \rangle \propto \sqrt{C}$  at a fixed  $\tau_Q$ . However, at small size  $C < 10\xi$ ,  $\langle |W| \rangle \propto \tau_Q^{-0.2}$  at fixed  $C$  and  $\langle |W| \rangle \propto C^{0.8}$  at a fixed  $\tau_Q$ . Now a theoretical model and even a numerical simulation is still lacking to address the experimental observation. Also, the KZM does not include the case when the system size is not an integer multiple of  $\xi$  since at large sizes the remainder can be ignored, the number of KZM pieces  $N$  is always an integral. However, at a finite size close to

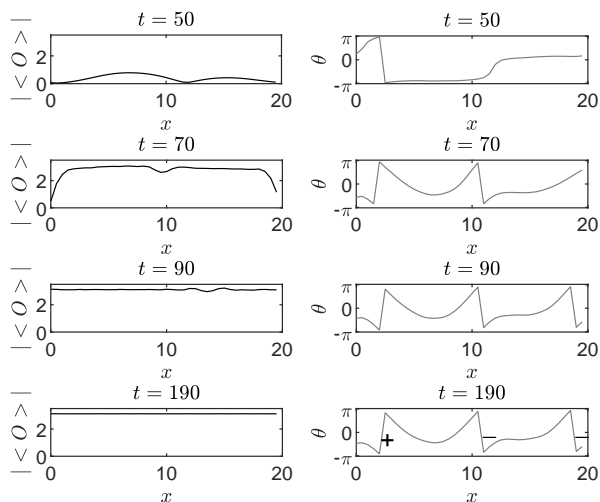


FIG. 1. **Winding up a superconducting ring after a temperature quench**  $\tau_Q = e^3$ , the circumference  $C = 20$ . In the four rows we show the magnitude of the order parameter  $|\langle O \rangle|$  and its phase  $\theta$  configuration in the dynamic process. The system finally enters an equilibrium state with constant amplitude of order parameter and a fixed configuration of phase field  $\theta(x)$ . The winding number  $W = n^+ - n^- = -1$ ,  $n^+ = 1$ ,  $n^- = 2$ .

$\xi$ , one have to consider the case of a fractional  $N$ . Furthermore, equilibrium phase transitions at finite size can still have universal scaling laws, as confirmed in a  $^3\text{He}$  superfluid phase transition [34] and a strongly coupled holographic superconductor [35], then it is of importance to study the finite size effect on dynamics and defects formation in phase transitions crossed at a finite rate.

In order to study the finite size Kibble-Zurek mechanism, we adopt a holographic superconductor ring model in the framework of Gauge/Gravity duality, focusing on the spontaneous formation of winding in the superconducting ring with any value of circumference after a temperature quench. The Gauge/Gravity duality[36–38] that relates strongly interacting quantum field theories to theories of classic gravity in higher dimensions has been proved to be a new and useful scheme to study strongly interacting condensed matter systems in equilibrium[39, 40], and also to study the real time dynamics when the system is far away from equilibrium [41–43]. Then it is very suitable to study the phase transition dynamics happened at a finite rate[14–16, 44–49]. We adopt the well studied holographic superconductor model defined in a AdS black hole [50–52],

$$S = \int d^4x \sqrt{-g} \left[ -\frac{1}{4} F^2 - (|D\Psi|^2 - m^2 |\Psi|^2) \right]. \quad (3)$$

This is the Einstein-Maxwell-complex scalar model, where the black hole background geometry is  $ds^2 = \frac{\ell^2}{z^2} (-f(z)dt^2 - 2dtdz + dx^2 + dy^2)$  in the Eddington coordinate,  $f(z) = 1 - (z/z_h)^3$ , the black hole temperature

$T = 3/(4\pi z_h)$ .  $x, y$  are the boundary spatial coordinates. There is a critical value of the black hole temperature below that the charged scalar develops a finite value in the bulk while its dual field theory operator have a finite expectation value  $\langle O \rangle$ , which breaks the  $U(1)$  symmetry in the boundary field theory. Working in 1D spatial boundary geometry by only turning on coordinate  $x$  dependence of all the fields in the equations of motion, using the periodic boundary condition in the  $x$  coordinate we are effectively studying a superconducting ring. By solving the dynamic equations by changing the black hole temperature above  $T_c$  to a one below  $T_c$ , the quench induced winding number formation process can be monitored in details[53]. One sample result of a quench from  $1.1T_c$  to  $0.82T_c$  is given in Fig.1, where  $\tau_q = e^3$  and  $C = 20$ . After the quench the order parameter amplitude approaches the equilibrium value while the phase develops a stable configuration that does not change anymore, the winding number  $W = -1$ . From the phase configuration in Fig.1, we can define the number of local positive winding numbers  $n^+$  and also the number of local negative winding numbers  $n^-$  as shown in the last plot, then  $W = n^+ - n^- = 1 - 2 = -1$ . The  $n^+$  and  $n^-$  are important to understand the statistics of  $W$  as will be shown later.

The winding number  $W$  of a long quenched superconducting ring admits a Gaussian distribution then its average value is always zero [13]. In order to see how quench rate affect the formation of  $W$ , people always refer to its variance  $\sigma^2(W)$ , which is proportional to the number of independent pieces  $N = C/\xi \propto \tau_q^{-1/4}$  using the mean field exponents  $z = 2$  and  $\nu = 1/2$  in Eq.(1),  $\xi$  is the correlation length corresponding to the time when the frozen time end. At large  $N$  limit, the mean absolute winding number  $\langle |W| \rangle$  can be computed from the Gaussian distribution, then one can obtain the key prediction [13]

$$\sigma(W) = \sqrt{\langle W^2 \rangle} \propto \langle |W| \rangle \propto \tau_Q^{-1/8}. \quad (4)$$

At a fixed rate, one can have  $\langle |W| \rangle \propto \sigma(W) \propto \sqrt{N}$ .

Fig.2 (left) plots  $\sigma^2(W)$  as a function of  $C$  for four different quench rates ( $\tau_Q = e^4, e^5, e^6, e^7$ ), average over 100000 times calculation for a circumference. According to KZM, since the system inherits an infinite relaxation time at the critical point then it can not catch the speed of a quench, as a result, the superconducting ring will be divided into many independent pieces with their average size to be  $\xi(\tau_Q)$ . The topological defects forms at the positions where the independent pieces meet, it is nature to conclude that there will be a critical value of circumference  $\tilde{C}$  that below which there is only one piece then no winding number will be formed.  $\tilde{C}$  is the average size of an independent region, also the value of the correlation length  $\xi(\tau_Q)$ . Numerical result of  $\tilde{C}$  confirmed the key prediction of KZM that  $\xi(\tau_Q) \propto \tau_Q^{1/4}$  (Fig.2 inset).

The Log-Log plot finds that the slope  $k = 0.224$ , close to 0.25 as expected. According to KZM's picture of the quenched dynamic phase transition,  $\sigma^2(W)[C]$  lines for different rates can be scaled to exactly one line by transforming  $C$  to be the number of regions/pieces formed (Fig.2 (right)), in a formula it can be expressed as

$$\sigma^2(W_{\tau_{Q1}})[C_1] = \sigma^2(W_{\tau_{Q2}})[C_2], \quad (5)$$

when  $C_1/\xi(\tau_{Q1}) = C_2/\xi(\tau_{Q2}) = N$ ,  $N$  is the number of independent pieces formed after the quench. Also the linear relationship  $\sigma^2(W) \propto N$  between variance of winding number and number of regions can be seen when the size of regions is roughly larger than five. Then, we confirmed the KZM mechanism from another perspective from the size dependent results rather than computing Eq.(2) directly. Note that the agreement also confirmed the fact that a holographic superconducting phase transition is always of the mean field class [54–56].

Besides the perfectly KZM matched results, from Fig.(2) one can also find that the prediction  $\sigma^2(W) \propto N$  can not hold when the ring size is reducing. From Fig.(3) (b) the log-log plot tells that the non KZM region is  $1 < N \leq 5$ . Also in this region, there is another interesting feature that  $\sigma^2(W) = \langle |W| \rangle$ , since the winding number can have only three value  $-1, 0, 1$ . with the vanishing ( $W$ ). One thing needs to emphasize is that in this region, though the KZM pieces  $N$  can be larger than one,  $W$  does not take a value larger than one, this may indicates that the formation of topological defects in a size  $N \leq 5$  is effectively correlated.

Also from Fig.3 (b,c), at a larger size  $5 < N < 10$ ,  $\sigma^2(W)$  has a linear dependence of  $N$ , but

$$\langle |W| \rangle \propto N^{0.8}. \quad (6)$$

This is different from the large size result  $\langle |W| \rangle \propto N^{0.5}$ , which is a result that the  $W$  admit a Gaussian distribution [13]. Then one can conclude that the Gaussian distribution is not good any more to capture the statistic distribution of winding number at the small size case. We compared the discrete distribution and the corresponding Gaussian distribution with the variance of  $W$  in Fig.(4), which shows the winding distribution at three different numbers of regions  $N = 8, 18, 30$ . The discrete distribution approaching a Gaussian one when increasing  $N$ . While  $N < 10$ ,  $|W|$  has only three values from zero to two, the deviation from Gaussian distribution is expected. Combining Eq. 6 and

$$\xi = \frac{C}{N} \propto \tau_Q^{1/4}, \quad (7)$$

we get exactly the scaling between average absolute winding number and quench rate beyond KZM reported in experiment [31] when  $5 < N < 10$

$$\langle |W| \rangle \propto \tau_Q^{-0.2}. \quad (8)$$

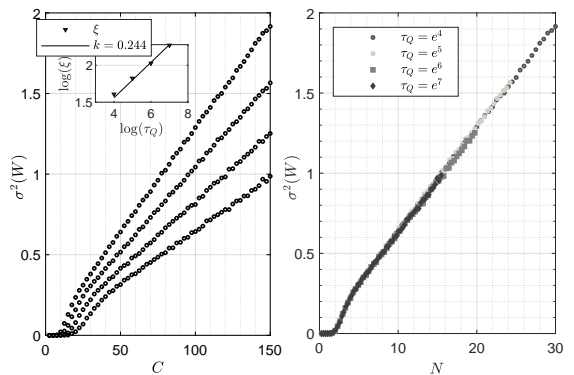


FIG. 2. **Size dependence of variance  $\sigma^2(W)$ .** (left) Size dependence of  $\sigma^2(W)$  for four quench rates, from top to bottom,  $\tau_Q = e^4, e^5, e^6, e^7$ . The inset shows the scaling of the critical circumference. (right)  $\sigma^2(W)$  as a function of pieces number  $N$ , all quench rate results are identical to each other.

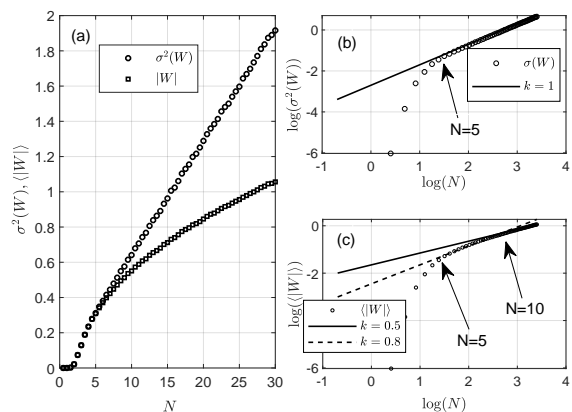


FIG. 3. **Scaling of  $\sigma^2(W)$  and  $\langle |W| \rangle$ .** (a)  $\sigma^2(W)$  and  $\langle |W| \rangle$  as a function of  $N$ , when  $N < 5$  the two have the same values. (b) Logarithmic relationship between  $\sigma^2(W)$  and  $N$ . (c) Logarithmic relationship between  $\langle |W| \rangle$  and  $N$ .  $k$  is the linear fit slope.

Due to the fact that the global winding number  $W = n^+ - n^-$ , the winding number in local regions can be  $+$ ,  $-$  or  $0$ , it is nature to expect the distribution of local winding number  $n^+, n^-$  can be captured by a trinomial distribution. The probability of the trinomial distribution of trials  $\tilde{N}$  reads

$$P(\tilde{N}, n^+, n^-) = \frac{\tilde{N}!}{n^0!n^+!n^-!} \left(\frac{p}{2}\right)^{n^++n^-} (1-p)^{n^0}, \quad (9)$$

where  $n^0 = \tilde{N} - (n^+ + n^-)$ ,  $n^0$  is the number of pieces where there is no local winding number.  $(n^+, n^-, n^0) \leq \tilde{N}$ ,  $\tilde{N}$  equals to largest number of  $n^+(n^-)$ , which can be defined as the number of effectively unrelated pieces.  $p/2$  is the probability for both “+” and “-” since the two have the same distribution [57], while  $1 - p$  is the

“0” probability. From the largest number of  $n^+(n^-)$  of a fixed  $N$  we find that  $\tilde{N} = n_{max}^+ = N/5$ . Furthermore, we consider the case when the  $\tilde{N}$  is not a integral, by increasing from  $\tilde{N}$  from a smaller integral number  $M$  to  $M + 1$ , the  $\sigma^2(W)$  is increasing continuously without a jump. To understand the continuous of  $\sigma^2(W)$ , we apply the mathematical theorem that the factorial in Eq.(9) can be expressed by the Gamma function

$$M! = \Gamma(M + 1) = \int_0^\infty y^M e^{-y} dy. \quad (10)$$

To understand the fractional number  $N$  of KZM pieces formed after a quench, we conject that the number of pieces formed admit a normal distribution with it's average value equal to  $N$ , which can be a any value fractional number. With the distribution, one can calculate the probability  $P(|W|)$ , for example,  $P(W = 0)$  is the summation of the cases where  $n^+ = 0, n^- = 0$  and  $n^+ = n^-$  in Eq.(9).  $P(|W| = 1)$  equals to the summation of the cases where  $n^+ = n^- \pm 1$ .  $P(|W|)$  as a function of  $\tilde{N} = N/5$  obtained from the trinomial distribution can basically match the numerical results as shown in Fig. 4 (d), the best fit parameters were found to be  $p = 0.324$  and  $\tilde{N} = N/5$ , due to the fact that when  $N = 30$ ,  $|W|$  has it's maximal value  $|W|_{max} = 6$ . The  $P(|W| = 0)$  will keep decreasing when  $|W|$  takes larger maximal values due to the increasing numbers of pieces.  $P(|W| = 1) = 0$  when  $N < 1$ , when  $N > 1$   $P(|W| = 1)$  keeps increasing to its maximal value at about  $\tilde{N} = 2$ .  $P(|W| = 2) = 0$  when  $N < 5$  ( $\tilde{N} < 1$ ). In a word,  $P(|W| = M)$  will have a finite value only when  $N > 5M$  ( $\tilde{N} > M$ ). Another check of the trinomial distribution can be done by computing  $\sigma^2(W)$  and  $\langle |W| \rangle$  from  $P(W)$  obtained from Eq.(9) [58], compare the results to the numerical simulation in Fig. 3 we find good agreement when  $\tilde{N} \geq 2$ . The deviation is obvious when  $\tilde{N} < 1$ , in this region with only one effectively independent KZM piece, there are only three possibilities:  $n^+ = n^- = 0; n^+ = 1, n^- = 0$ ; and  $n^+ = 0, n^- = 1$ . Then  $\langle |W| \rangle = \sigma^2(W) = P(n^+ = 1) + P(n^- = 1) = p$ , the probability  $p$  is increasing from zero at  $N = 1$  to a constant  $p = 0.324$  at  $N = 5$ .

In summary, our numerical experiment on spontaneous formation of winding numbers in a finite size ring not only confirms the KZM predictions but also presents new findings of dynamics of phase transition in a superconducting ring. Firstly, the finite size distribution of  $W$  is different from Gaussian distribution then the KZM scaling law of  $\langle |W| \rangle$  will be modified, which agrees the experimental observation [33]. Secondly, the KZM assumes the pieces formed after a quench are independent, while the numerical results at finite size indicates that the five adjacent pieces are correlated, then the effective independent pieces  $\tilde{N} = L/5\xi$ . Furthermore, a continuous version of trinomial distribution with a fractional  $\tilde{N}$  trial was proposed to understand the size dependent statistic distribution of winding numbers. The nonlinear dependence

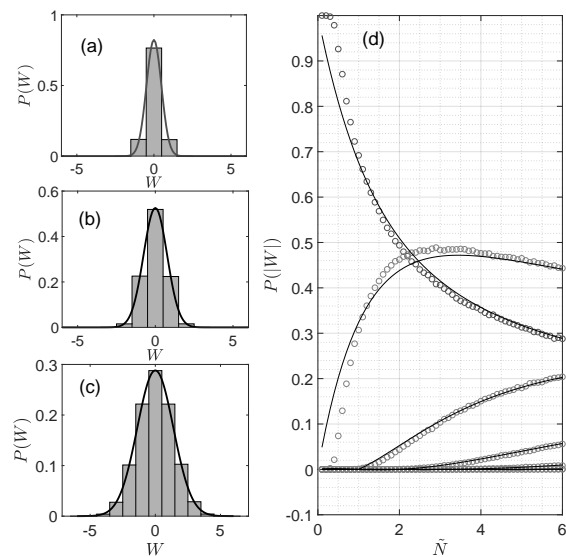


FIG. 4.  $P(\langle |W| \rangle)$  from trinomial distribution. (a-c) Histogram of  $P(W)$  for  $N = 8, 18, 30$  respectively when  $\tau_Q = e^4$ . (d) Numerical results of  $P(|W|)$  (circles, from top to bottom are  $|W| = 0, 1, 2, 3, 4, 5, 6$  respectively) and their fitted curves from Eq.8 (Solid lines).

between  $\sigma^2(W)$  and  $N$  is believed to be a results that the winding number formation process are dependent when  $N \leq 5$ , where the probability  $p$  equals to  $\sigma^2(W)$  which is  $C$  dependent. The number of effectively independent pieces is  $\tilde{N} = N/5$ , where  $\tilde{N}$  still admits the scaling law predicted by Kibble-Zurek mechanism.

*Acknowledgements.*— We thank Wei Can Yang for valuable discussions. This work is supported by the National Natural Science Foundation of China (under Grant No. 11675140).

- 
- [1] T. W. B. Kibble, J. of Phys. A: Math. Gen. **9**, 1387 (1976).
  - [2] T. W. B. Kibble, Physics Reports **67**, 183 (1980).
  - [3] W. H. Zurek, Nature **317**, 505 (1985).
  - [4] W. H. Zurek, Acta Phys. Pol. B **24**, 1301 (1993).
  - [5] W. H. Zurek, Physics Reports **276**, 177 (1993)
  - [6] J. Dziarmaga, Advances in Physics **59**, 1063 (2010).
  - [7] A. Polkovnikov, K. Sengupta, A. Silva, and M. Vengalattore, Rev. Mod. Phys. **83**, 863 (2011).
  - [8] A. del Campo and W. H. Zurek, International Journal of Modern Physics A **29**, 1430018 (2014).
  - [9] N. D. Antunes et al., Phys. Rev. Lett. **82**, 2824 (1999).
  - [10] M. B. Hindmarsh and A. Rajantie, Phys. Rev. Lett. **85**, 4660 (2000).
  - [11] Andrew Yates, and Wojciech H. Zurek, Phys. Rev. Lett. **80**, 5477 (1998).
  - [12] Pablo Laguna, and Wojciech Hubert Zurek, Phys. Rev. Lett. **78**, 2519 (1996).
  - [13] A. Das, J. Sabbatini and W. H. Zurek, Sci. Rep. **2**, 352

- (2012).
- [14] J. Sonner, A. del Campo and W. H. Zurek, *Nature Commun.* **6**, 7406 (2015)
- [15] P. M. Chesler, A. M. Garcia-Garcia and H. Liu, *Phys. Rev. X* **5**, no. 2, 021015 (2015).
- [16] Hua-Bi Zeng, Chuan-Yin Xia, Wojciech H. Zurek, Hai-Qing Zhang, arXiv:1912.08332 [hep-th].
- [17] I. Chuang, B. Yurke, R. Durrer and N. Turok, *Science* **251**, 1336 (1991).
- [18] M. J. Bowick, L. Chandar, E. A. Schik and A. M. Srivastava, *Science* **263** 943 (1994).
- [19] S. Digal, R. Ray and A. M. Srivastava, *Phys. Rev. Lett.* **83**, 5030 (1999).
- [20] C. Baeuerle, Y. M. Bunkov, S. N. Fisher, H. Godfrin and G. R. Pickett, *Nature* **382**, 332 (1996).
- [21] V. M. H. Ruutu et al., *Nature* **382**, 334 (1996).
- [22] R. Carmi, E. Polturak and G. Koren, *Phys. Rev. Lett.* **84**, 4966 (2000).
- [23] R. Monaco, J. Mygind and R. J. Rivers, *Phys. Rev. Lett.* **89**, 080603 (2002).
- [24] R. Monaco, J. Mygind, and R. J. Rivers, *Phys. Rev. B* **67** 104506 (2003).
- [25] R. Monaco, J. Mygind, M. Aaroe, R. J. Rivers and V. P. Koshelets, *Phys. Rev. Lett.* **96** 180604 (2006).
- [26] A. Maniv, E. Polturak and G. Koren, *Phys. Rev. Lett.* **91**, 197001 (2003).
- [27] D. Golubchik, E. Polturak, G. Koren, *Phys. Rev. Lett.* **104**, 247002 (2010).
- [28] X.-Y. Xu, Y.-J. Han, K. Sun, J.-S. Xu, J.-S. Tang, C.-F. Li and G.-C. Guo, *Phys. Rev. Lett.* **112**, 035701 (2014).
- [29] B. Ko, J. W. Park, and Y. Shin, *Nat. Phys.* **15**, 1227 (2019).
- [30] A. del Campo, *Phys. Rev. Lett.* **121**, 200601 (2018).
- [31] F. J. Gomez-Ruiz, J. J. Mayo, A. del Campo, *Phys. Rev. Lett.* **124**, 240602 (2020).
- [32] J.-M. Cui, F. J. Gomez-Ruiz, Y.-F. Huang, C.-F. Li, G.-C. Guo, and A. del Campo, *Comm. Phys.* **3**, 44 (2020).
- [33] L. Corman, L. Chomaz, T. Bienaime, R. Desbuquois, C. Weitenberg, S. Nascimbene, J. Dalibard, and J. Beugnon, *Phys. Rev. Lett.* **113**, 135302 (2014).
- [34] Francis M. Gasparini, Mark O. Kimball, Kevin P. Mooney, and Manuel Diaz-Avila, *Rev. Mod. Phys.* **80**, 1009 (2008).
- [35] Antonio M. Garca-Garca, Jorge E. Santos, and Benson Way, *Phys. Rev. B* **86**, 064526 (2012).
- [36] J. M. Maldacena, *Adv. Theor. Math. Phys.* **2**, 231 (1998).
- [37] S. S. Gubser, I. R. Klebanov, and A. M. Polyakov, *Phys. Lett. B* **428**, 105 (1998).
- [38] E. Witten, *Adv. Theor. Math. Phys.* **2**, 253 (1998).
- [39] J. Zaanen, Y. W. Sun, Y. Liu and K. Schalm, “Holographic Duality in Condensed Matter Physics,” Cambridge University Press, 2015.
- [40] M. Ammon and J. Erdmenger, “Gauge/gravity duality: Foundations and applications,” Cambridge University Press, 2015.
- [41] H. Liu and J. Sonner, arXiv:1810.02367 [hep-th].
- [42] A. Adams, P. M. Chesler, and H. Liu, *Science* **341**, 368 (2013).
- [43] W. J. Li, Y. Tian, and H. B. Zhang, *J. High Energy Phys.* **07** (2013) 030.
- [44] K. Murata, S. Kinoshita, and N. Tanahashi, *J. High Energy Phys.* **07** (2010) 050.
- [45] M. J. Bhaseen, J. P. Gauntlett, B. D. Simons, J. Sonner, and T. Wiseman, *Phys. Rev. Lett.* **110**, 015301 (2013).
- [46] M. Natsuume and T. Okamura, *Phys. Rev. D* **95** 106009 (2017).
- [47] S. R. Das and T. Morita, *J. High Energy Phys.* **01** (2015) 084.
- [48] P. Basu and S. R. Das, *J. High Energy Phys.* **01** (2012) 103.
- [49] Basu, D. Das, S. R. Das and T. Nishioka, *J. High Energy Phys.* **03** (2013) 146.
- [50] S. S. Gubser, *Phys. Rev. D* **78**, 065034 (2008).
- [51] S. A. Hartnoll, C. P. Herzog, and G. T. Horowitz, *Phys. Rev. Lett.* **101**, 031601 (2008).
- [52] C. P. Herzog, P. K. Kovtun and D. T. Son, *Phys. Rev. D* **79**, 066002 (2009).
- [53] See Supplemental Material for the equation of motion and the numerical scheme to simulate a temperature quench.
- [54] K. Maeda, M. Natsuume, and T. Okamura, *Phys. Rev. D* **79**, 126004 (2009).
- [55] K. Jensen, *Phys. Rev. Lett.* **107**, 231601 (2011).
- [56] H. B. Zeng, H. Q. Zhang, *Phys. Rev. D* **98**, 106024 (2018).
- [57] See Fig.5 in the Supplemental Material for the distribution of  $n^+$  and  $n^-$  at three different sizes,  $P(n^+)$  always equals to  $P(n^-)$ .
- [58] See Fig.6 in the Supplemental Material for the plots of  $\sigma^2(W)$  and  $\langle |W| \rangle$  obtained from trinomial distribution and dynamic simulation.

## SUPPLEMENTAL MATERIAL

## Equation of motion and the numerical scheme to simulate a temperature quench

With the ansatz  $\Psi = \Psi(t, z, x)$ ,  $A_t = A_t(t, z, x)$ ,  $A_x = A_x(t, z, x)$ ,  $A_y = A_z = 0$ , and define  $\Phi = \Psi/z$ . The implicit form of the Euler-Lagrange equations from Einstein-Maxwell-complex scalar model reads

$$\partial_t \partial_z \Phi - i A_t \partial_z \Phi - \frac{1}{2} [i \partial_z A_t \Phi + f \partial_z^2 \Phi + f' \partial_z \Phi - z \Phi + (\partial_x^2 \Phi) - i \partial_x A_x \Phi - A_x^2 \Phi - 2i(A_x \partial_x \Phi)] = 0; \quad (11)$$

$$\partial_t \partial_z A_t - (\partial_x^2 A_t + \partial_y^2 A_t) - f \partial_z (\partial_x A_x + \partial_y A_y) + \partial_t (\partial_x A_x + \partial_y A_y) + 2A_t |\Phi|^2 - i f (\Phi^* \partial_z \Phi - \Phi \partial_z \Phi^*) + i (\Phi^* \partial_t \Phi - \Phi \partial_t \Phi^*) = 0; \quad (12)$$

$$\partial_t \partial_z A_x - \frac{1}{2} [\partial_z (\partial_x A_t + f \partial_z A_x) - i (\Phi^* \partial_x \Phi - \Phi \partial_x \Phi^*) - 2A_x |\Phi|^2] = 0; \quad (13)$$

There is another constrain equation from the time component of Maxwell equations,

$$\partial_z (\partial_x A_x - \partial_z A_t) + i (\Phi^* \partial_z \Phi - \Phi \partial_z \Phi^*) = 0. \quad (14)$$

Throughout this paper, we work in the units with  $e = c = \hbar = k_b = 1$  and we also have scaled  $\ell = 1$ .

There is a critical black hole temperature below which the solution with a finite  $\Phi$  then the  $U(1)$  symmetry can be spontaneous broken, all the critical exponents at the phase transition point are of the standard mean field values.

To solve the highly non-linear PDEs, the boundary condition for the charged scalar and the gauge field must be imposed, specifically, at the infinite boundary,

$$A_x(t, z, x) = a_x(t, x) + b_x(t, x)z + \mathcal{O}(z^2), \quad (15)$$

$$\Psi(t, z, x) = \Psi_1(t, x)z + \Psi_2(t, x)z^2 + \mathcal{O}(z^3). \quad (16)$$

from the AdS/CFT correspondence dictionary the coefficients  $a_x$  can be regarded as the gauge field on the boundary along  $x$  directions while  $J_x = -b_x - (\partial_x a_t - \partial_t a_x)$  is the supercurrent. By fixing  $J_x$  we are dealing with a superconducting ring with dynamic gauge field  $a_x$  [1–4]. Coefficients  $a_t$  and  $b_t$  are interpreted as chemical potential  $\mu$  and charge density  $\rho$  respectively in the boundary field theory. Moreover,  $\Psi_1$  is a source term which is set to be zero, then  $\Psi_2$  is the vacuum expectation value  $\langle O \rangle$  of the dual scalar operator in the boundary in the spontaneous symmetry broken phase. The temperature of the black hole is  $T = 3/(4\pi z_h)$ , technically, to tune the temperature people usually set  $z_h = 1$  while changing the value of  $\rho$  according a scale symmetry of the equation. The dimensionless quantity relate temperature and the  $\rho$  is  $T/\rho^2$ , there is critical  $\rho_c \approx 4.06$  above which the system

will enter a lower free energy state with non-vanishing  $\Psi$ , quenching a  $\rho$  across  $\rho_c$  is equal to quench the system from a high temperature state to a low temperature state in a linear way by the following setup of a time dependent  $\rho(t)$  in the quenching stage before approaching the final temperature  $T_f < T_c$

$$\rho(t) = \rho_c (1 - \frac{t}{\tau_Q})^{-2}. \quad (17)$$

$t = 0$  is defined as the moment quench begins, before quenching the superconductor, the system with initial fluctuations had been thermalized for a sufficient time. The initial random seeds of the fields in the bulk by satisfying the statistical distributions  $\langle s(t, x_i) \rangle = 0$  and  $\langle s(t, x_i) s(t', x_j) \rangle = h \delta(t - t') \delta(x_i - x_j)$ , with the amplitude  $h = 10^{-3}$ . In the radial direction  $z$ , we use the Chebyshev pseudo-spectral method with 21 grids. Since in the  $x$ -directions, all the fields are periodic, we use the Fourier decomposition along  $x$ -directions. Filtering of the high momentum modes are implemented following the “2/3’s rule” that the uppermost one third Fourier modes are removed [5].

- 
- [1] K. Skenderis, Class. Quant. Grav. 19, 5849 (2002).
  - [2] E. Witten, SL(2,Z) action on three-dimensional conformal field theories with Abelian symmetry, In \*Shifman, M. (ed.) et al.: From fields to strings, vol. 2\* 1173-1200.
  - [3] O. Domenech, M. Montull, A. Pomarol, A. Salvio and P. J. Silva, JHEP 1008, 033 (2010).
  - [4] M. Montull, A. Pomarol and P. J. Silva, Phys. Rev. Lett. **103**, 091601 (2009).
  - [5] P. M. Chesler and L. G. Yaffe, JHEP 1407, 086 (2014).

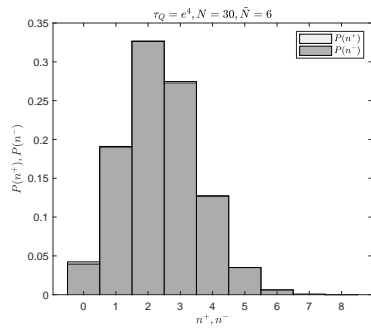
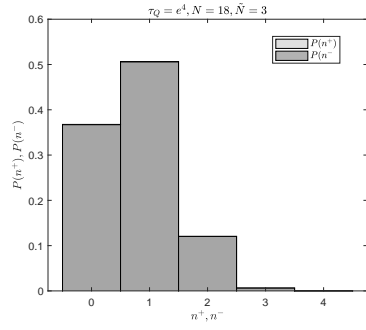
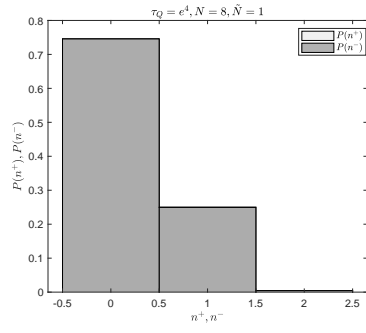


FIG. 5. Distribution of  $n^+$  and  $n^-$  for three different sizes.  $P(n^+)$  always equals to  $P(n^-)$ .

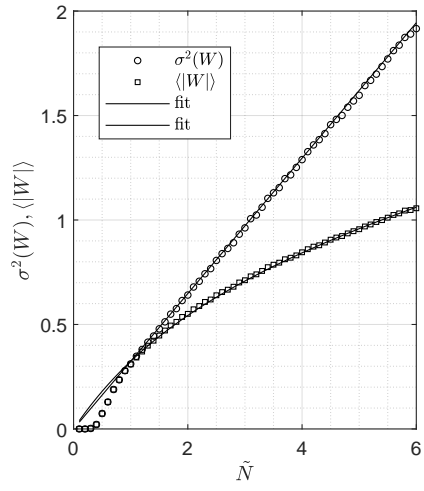


FIG. 6.  $\sigma^2(W)$ ,  $\langle |W| \rangle$  and their fitted curves from trinomial distribution.